DOI: 10.1002/chem.200601188

Controlling the Confinement and Alignment of Fullerene C_{70} in *para*-Substituted Calix[5]arenes

Mohamed Makha, Joshua J. McKinnon, Alexandre N. Sobolev, Mark A. Spackman, and Colin L. Raston*[a]

Abstract: In toluene fullerene C_{70} forms 2:1 complexes with *p*-benzylcalix[5]arene (**1**) and *p*-phenylcalix[5]arene (**2**), $[C_{70}\subset\mathbf{1}_2]\cdot 6(C_7H_8)$ and $[C_{70}\subset\mathbf{2}_2]\cdot 7(C_7H_8)$. The fullerene molecules are completely shrouded by two calix[5]arenes in addition to terminal benzyl groups from other supermolecules, $[C_{70}\subset\mathbf{1}_2]$, and solvent. Within the capsule-like supermolecules the calixarenes have distinctly different arrangements relative to the principal axis of the fullerene; for $[C_{70}\subset\mathbf{1}_2]\cdot 6(C_7H_8)$ the oxygen planes of the two calixarenes are skewed by 37.0 and 47.5°, whereas in $[C_{70}\subset\mathbf{2}_2]\cdot 7(C_7H_8)$ the principal axes of the fullerene and the two encapsulating calixarenes are more closely aligned with the corresponding angles at 9.7 and 8.6°, and features a pentaphenyl inter-calixarene embrace. The Hirshfeld surfaces of these two complexes have been investigated for a detailed understanding of the orientation and nature of interactions of C_{70} with the cavitand-type molecules and toluene.

Keywords: calixarenes · fullerenes · Hirshfeld surfaces · self-assembly · supramolecular chemistry

The ability to control the encapsulation of fullerene C_{60} by one or more host molecules is well documented as is the control of the interplay of fullerene C_{60} molecules into continuous arrays using host–guest chemistry.[1] In the case of C_{70} the ability to control both encapsulation and interplay of the fullerene is developing, and appears to be problematic.[2] This is highlighted by the recent structural authentication of the C_{70} complex with the oligophenolic macrocycle *p*-*t*Bu-calix[6]arene where the fullerene does not reside in the cavity of the calixarene,[2] which is at odds with earlier predictions.[3] Difficulties in predicting the nature of complexes of C_{70} with host molecules are associated with the larger size of the fullerene and its shape anisotropy which is relayed in inefficiencies in its packing in continuous structures containing fullerene···fullerene interactions.

p-Benzylcalix[5]arene (**1**) and *p*-phenylcalix[5]arene (**2**) are bowl-shaped molecules possessing hydrophobic cavities having size and shape complementarity relative to C_{60}, and their process in binding this fullerene has been established both in solution and in the solid state.[4–6] Calix[5]arene **1** with its dangling benzyl groups forms 1:1 and 2:1 supermolecules in toluene, crystallising as the 2:1 complex, $[C_{60}\subset\mathbf{1}_2]\cdot 8(C_7H_8)$, where the fullerene is shrouded by two calixarenes, centred 180° apart, and solvent molecules.[4,5] The rigid extended phenyl groups in calixarene **2** creates a deeper cavity and in the solid state a 2:1 complex forms, $[C_{60}\subset\mathbf{2}_2]\cdot 1.5(C_7H_8)$, with most of the surface of the C_{60} shrouded by two calixarenes but these are now centred 157.5° apart with the phenyl groups interdigitated in one hemisphere of the supermolecule.[6] The host–guest interplay between C_{60} and **1** and **2** in their cone conformations involves π···π interactions made possible by the complementarity of curvature of the two components. In addition, the alignment of the C_5 symmetry axis of the calix[5]arene in **1** in the cone conformation with a C_5 symmetry axis of electron deficient C_{60} is favoured energetically.[5] In the case of **2** the non-linear arrangement of the calixarenes results in the fullerene being "confused", and this is manifested in the C_{60} molecule being disordered.[5]

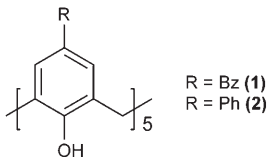

As part of a systematic study on the interplay of fullerene C_{70} with container molecules we have investigated the complexation of the fullerene with the same calixarenes, **1** and

[a] Dr. M. Makha, Dr. J. J. McKinnon, Dr. A. N. Sobolev, Prof. M. A. Spackman, Prof. C. L. Raston
School of Biomedical, Biomolecular and Chemical Sciences
The University of Western Australia, 35 Stirling Hwy, Crawley
WA 6009 (Australia)
Fax: (+61) 8-6488-1005
E-mail: clraston@chem.uwa.edu.au

2, in the same solvent as for the corresponding studies for C_{60}, namely toluene. This offers scope for a direct comparison between the two fullerenes, in determining the effect of different size and shape of the fullerenes, and any orientation effects of the C_{70} molecules.

Attempts in establishing the nature of the host–guest species present in toluene solutions of either calixarene **1** or **2** with fullerene C_{70} were unsuccessful. In the solid state, however, we have isolated and structurally authenticated a 2:1 complex for each calixarene, respectively $[C_{70}\subset\mathbf{1}_2]\cdot 6(C_7H_8)$ and $[C_{70}\subset\mathbf{2}_2]\cdot 7(C_7H_8)$. In both complexes the C_{70} molecules are shrouded by two container molecules, but the orientation of the calixarenes relative to each other within each supermolecule is distinctly different to that in the corresponding supermolecules for the fullerene C_{60} complexes.[4,6] These C_{70} complexes represent the simplest case for the supramolecular chemistry of the fullerene, where the fullerene is devoid of any fullerene···fullerene interactions. Herein we also report a detailed study of the Hirshfeld surfaces of these two complexes, as a starting point for understanding the orientation and interplay of C_{70} with cavitand-type molecules, with a view that this approach can be extended to C_{76} and higher fullerenes. In general, Hirshfeld surfaces[7,8] and related graphical tools[9,10] provide a means of exploring the nature of the intermolecular interactions between molecules. Generating Hirshfeld surfaces is now possible for disordered systems, as for the disordered C_{70} molecules in $[C_{70}\subset\mathbf{1}_2]\cdot 6(C_7H_8)$.

Results and Discussion

Advances in the preparation of deep cavity phenyl- and benzylcalixarenes using benign synthetic methologies[11] have facilitated exploring their host–guest chemistry with a variety of globular guest molecules.[12] Slow evaporation of toluene solutions of *p*-benzylcalix[5]arene (**1**) and *p*-phenylcalix[5]arene (**2**) with half an equivalent of C_{70} in toluene, as a saturated solution of the fullerene, afforded hexa- and heptatoluene solvates, respectively, $[C_{70}\subset\mathbf{1}_2]\cdot 6(C_7H_8)$ and $[C_{70}\subset\mathbf{2}_2]\cdot 7\ (C_7H_8)$. The first omplex crystallizes in the monoclinic space group $P2_1/c$, $Z=4$, with the asymmetric unit comprised of one C_{70} fullerene encapsulated by two *p*-benzylcalix[5]arene molecules and six toluene molecules. The fullerene and two toluene molecules are disordered (50:50 ratio), the former being along its principal axis. All non-hydrogen atoms were refined anisotropically and H-atoms were calculated from geometrical considerations and constrained during refinement to the appropriate positional and thermal parameters of bonded C and O atoms. The C_{70} molecule resides unsymmetrically with respect to the cavity of the calixarene, the principal axis of the fullerene is canted relative the C_5 axis of the calixarenes at angles of 37.0 and 47.5°, respectively. In contrast the corresponding C_{60} complex of **1**, the C_5 axes of the calixarenes coincide with a C_5 axis of the fullerene.[4] This so-called "symmetry matching" of the components has been effective in preparing host–guest complexes of C_{60},[1] but clearly not so for the present C_{70} complexation.

Complex $[C_{70}\subset\mathbf{2}_2]\cdot 7(C_7H_8)$ crystallizes in the same space group, but with the principal axis of C_{70} almost aligned with the symmetry axis of each of the two calixarenes bound to the fullerene as depicted in Figure 1. In this complex the "symmetry matching" of the components has been effective, although for the corresponding C_{60} complex this is not the case (see below).[6] Here the asymmetric unit is this "molecular capsule"-like arrangement along with five toluene molecules which fill the space between the arms of the calixarenes, and two other solvate molecules. The two calixarenes and five toluene molecules effectively shroud the fullerene.

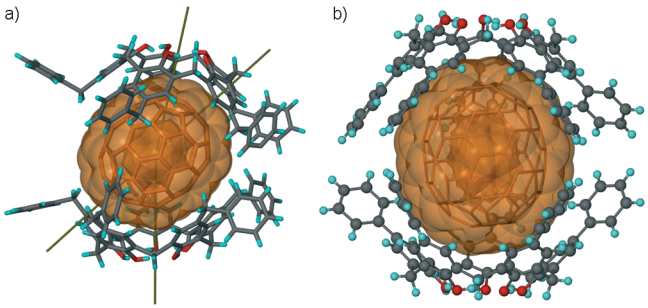

Figure 1. Projections of the supermolecules showing the orientation of C_{70} fullerene molecules: a) $[C_{70}\subset\mathbf{1}_2]\cdot 6(C_7H_8)$; b) $[C_{70}\subset\mathbf{2}_2]\cdot 7(C_7H_8)$ (toluene solvent molecules are omitted for clarity).

The calixarene molecules in both C_{70} complexes are arranged eclipsed relative to each other (see Figure 1 and see Hirshfeld surfaces below), which is distinctly different to the staggered arrangement in the analogous C_{60} complexes.[4,6] It is noteworthy that the staggered arrangement for the C_{60} complex of **1** is associated with the supermolecules residing on crystallographic inversion centres. The eclipsed arrangement is most striking in $[C_{70}\subset\mathbf{2}_2]\cdot 7(C_7H_8)$. The inclination of C_{70} and the skewing of the "molecular capsules" in $[C_{70}\subset\mathbf{1}_2]\cdot 6(C_7H_8)$ is ascribed to the calixarenes maximizing the interactive envelope around the fullerene C_{70}; the curvature of that part of the fullerene in the cavity of the calixarene still maintains complementarity of curvature of the components. Further inclination of the principal axis of the fullerene would distort the essentially symmetrical bowl shape of the lower rim of the calixarene. In this context we note that for the structure of the 1:1 complex of C_{70} with *para*-H-calix[5]arene, the angle between the principal axes of the two components is 40°,[13] although in this case fullerene···fullerene interactions present in the extended structure may perturb this angle. Even so the angle is within the two corresponding angles in the structure of $[C_{70}\subset\mathbf{1}_2]\cdot 6(C_7H_8)$.

The bowl-shape conformation of the calixarenes in both structures is related to the dihedral angles between the plane of the five oxygen atoms and the planes of the five phenolic rings in each calixarene. For $[C_{70}\subset\mathbf{1}_2]\cdot 6(C_7H_8)$

where the fullerene is disordered and less tightly confined by the calixarenes and solvent molecules, there is a spread of angles ranging from 131.0 to 139.6°, and 126.3 to 140.7° for the two calixarenes. For $[C_{70}\subset\mathbf{2}_2]\cdot 7(C_7H_8)$, the tightly shrouded fullerene is associated with a significantly smaller narrow distribution of angles, ranging from 131.1 to 138.5° and 133.7 to 139.0° for the two calixarenes.

The eclipsed arrangement of the calixarenes in the present complexes creates windows which are occupied by toluene solvent molecules for $[C_{70}\subset\mathbf{2}_2]\cdot 7(C_7H_8)$ while in complex $[C_{70}\subset\mathbf{1}_2]\cdot 6(C_7H_8)$, toluene molecules are concentrated on only one side of the hemispheric belt of the "molecular capsule". The difference relative to the C_{60} complexes relates to the difference in size and shape of the fullerenes. For calixarene **2** bound to spheroidal C_{60}, interdigitation of the *p*-phenyl substituents is possible, effectively shutting down any direct fullerene interaction with solvent molecules. This is unlike in the C_{70} complex where alignment of the fullerene along the axes of the calixarenes pushes the calixarenes sufficiently apart along the principal axis of the fullerene to allow intimate contact of the ends of the phenyl groups of one calixarene with the ends of the other calixarene while maintaining a snug fit of the fullerene inside the "molecular capsule". The interplay of the phenyl groups from the two calixarenes can be described as a pentaphenyl embrace which is related to the well known triphenyl embrace identified by Dance et al. for tetraphenyl phosphonium cations and related species.[14]

The overall packing in both structures features the columnar arrays of the capsular-like supermolecules with toluene molecules filling the interstitial space. The columnar arrays are stacked and are offset with respect to each other by one calixarene molecule. In $[C_{70}\subset\mathbf{1}_2]\cdot 6(C_7H_8)$, the columns are interlocked via the benzyl substituents directed to the hemispheric belt of another capsule as part of the complete encapsulation of each fullerene, and are also directed to the clefts at the base of the calixarenes. In $[C_{70}\subset\mathbf{2}_2]\cdot 7(C_7H_8)$ the stacking is simpler with no interplay of the arms of the calixarenes with other fullerene molecules. Full encapsulation of the fullerene also involves five toluene solvent molecules occupying the exposed gaps in the capsule (see Figure 2a and b), one having π···π interactions, whereas the other four have C-H···π interactions. C-H···π interactions involve methyl groups of some toluene molecules and the aromatic hydrogens of others with distances ranging from 3.09 to 3.18 Å, in addition to a π···π interaction involving the carbon of the six-membered rings of the fullerene and the aromatic ring of toluene with carbon···centroid short distance of 3.13 Å. Moreover, intricate hydrogen bonding between either the aromatic or methyl hydrogens of toluene with the phenyl of the calixarene are also found with short C−H···ring centroid distances of 2.8 Å.

The Hirshfeld surfaces[7,8] and related graphical tools[9,10] provide a means of exploring the nature of the intermolecular interactions between the calixarene, toluene and C_{70} molecules, and facilitate comparison between the two different supermolecules. The surface partitions space in the crystal into smooth non-overlapping volumes associated with each molecule. Inside the Hirshfeld surface the electron distribution due to a sum of spherical atoms for the molecule (the promolecule) dominates the corresponding sum over the crystal (the procrystal), and the Hirshfeld surface is defined implicitly where the ratio of promolecule to procrystal electron densities equals 0.5. Because the local nature of the surface is dictated by the proximity of all neighbouring atoms, both inside and outside the surface, it reflects in considerable detail the immediate environment of a molecule in a crystal, and summarizes all intermolecular interactions in a convenient graphical fashion. Figures 3–6 show various projections of the supermolecules for $[C_{70}\subset\mathbf{1}_2]\cdot 6(C_7H_8)$ and $[C_{70}\subset\mathbf{2}_2]\cdot 7(C_7H_8)$ with Hirshfeld surfaces mapped with d_e, the distance from the surface to the nearest nucleus external to the surface. Using a colour mapping which spans the range 1.0 Å (red) $\leq d_e \leq$ 2.5 Å (blue) for all surfaces shown, regions associated with close intermolecular contacts are identifiable as bright red spots on the surface, while regions associated with no close contacts are blue.

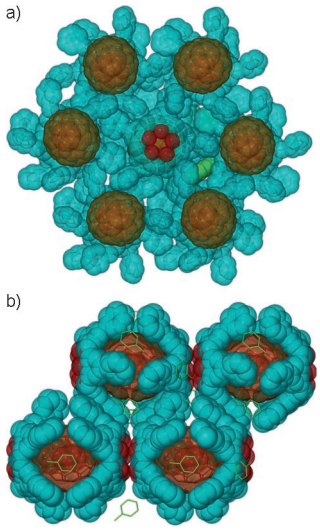

Figure 2. Projections of the packing diagram showing the assembly of columnar arrays in a) top view for $[C_{70}\subset\mathbf{1}_2]\cdot 6(C_7H_8)$; b) side view for $[C_{70}\subset\mathbf{2}_2]\cdot 7(C_7H_8)$ (toluene solvents molecules highlighted in green for clarity).

Figure 3 displays side-on projections of the two supermolecules, with front and back views for each. Hirshfeld surfaces are shown for both calixarene molecules and C_{70}, while the toluene molecules in close proximity are shown as tube models. The difference between the two supermolecules is immediately evident. In $[C_{70}\subset\mathbf{2}_2]\cdot 7(C_7H_8)$ calixarene molecules tightly encapsulate the fullerene, with eclipsed pendant arms on opposing calixarenes in close contact through numerous H···H interactions. The gaps between the pendant arms leave five windows which are occupied by solvent toluene molecules (one is disordered, see the right of Figure 3d); the remaining two toluene molecules occupy interstices between the supermolecules in the crystal. Figure 3 also clearly shows that the toluene molecules in the windows

of the structure are not simply occupying interstices—they are intimately involved in the supermolecular structure. That this is the case is evident from three of the toluene molecules visible in the windows in Figure 3c and d. The leftmost in Figure 3c is involved in a close π···π interaction with the fullerene, and at the same time several C-H···π donor interactions with the adjacent pendant arms of the calixarenes. The toluene on the right of Figure 3c (also visible on the left of Figure 3d) makes a single C-H···π donor contact, with the C–H bond pointing almost directly towards the centre of one of the six-membered rings of the fullerene; it also participates as a C-H···π acceptor in interactions with the calixarene arms. The toluene in the centre of Figure 3d makes two C-H···π contacts to the fullerene, one involving a hydrogen atom of the methyl group.

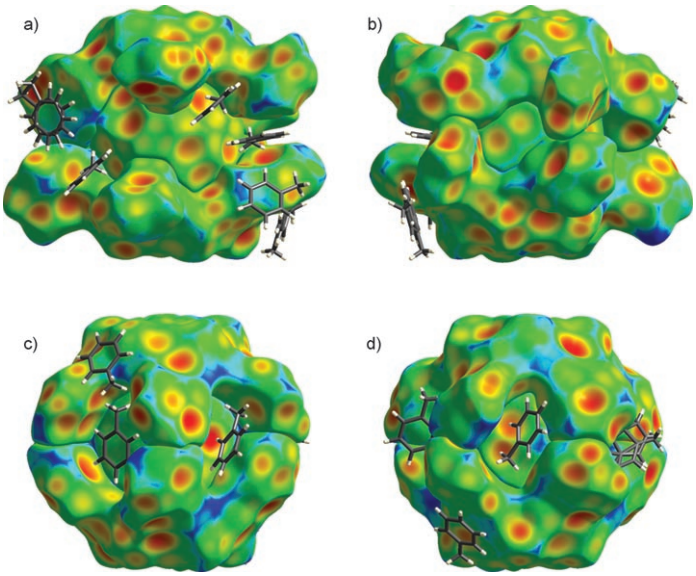

Figure 3. Hirshfeld surfaces for the "molecular capsules" in $[C_{70}\subset\mathbf{1}_2]\cdot 6(C_7H_8)$, (a) and (b), and $[C_{70}\subset\mathbf{2}_2]\cdot 7(C_7H_8)$, (c) and (d); toluene molecules are represented as tube models. The two views for each capsule are related by a 90° rotation about the vertical axis.

The importance of the solvent toluene molecules is most strikingly revealed in Figure 4, which depicts unit cell contents for $[C_{70}\subset\mathbf{2}_2]\cdot 7(C_7H_8)$, with toluene molecules represented by Hirshfeld surfaces mapped with d_e, fullerene molecules by plain, undecorated Hirshfeld surfaces, and calixarenes as tube models. The toluene molecules are not only intimately involved in the structure of the supermolecules, they participate in numerous C-H···π contacts with both the calixarene molecules and with one another, and these are quite obvious as red dots on the surfaces in the projection down the *a* axis.

In contrast with $[C_{70}\subset\mathbf{2}_2]\cdot 7(C_7H_8)$, the supermolecule in $[C_{70}\subset\mathbf{1}_2]\cdot 6(C_7H_8)$ is a much more open structure (Figure 3a and b). Whereas the calixarene molecules are eclipsed as in $[C_{70}\subset\mathbf{2}_2]\cdot 7(C_7H_8)$, their pendant arms make only tenuous contact with one another on one side of the supermolecule

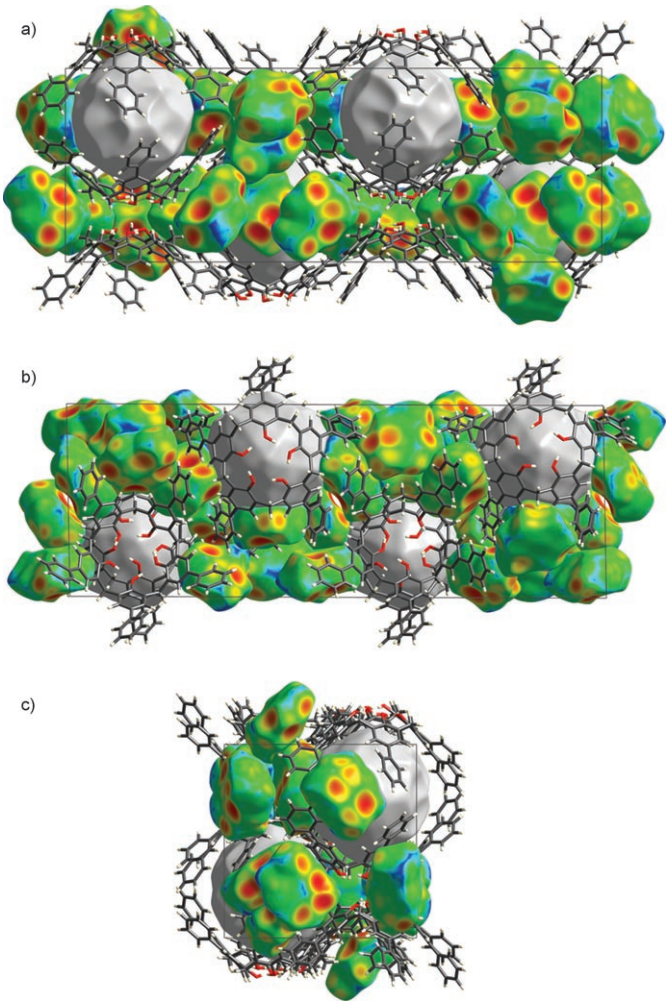

Figure 4. Unit cell contents for $[C_{70}\subset\mathbf{2}_2]\cdot 7(C_7H_8)$ projected down *a*, *b* and *c* cell axes. Toluene molecules are represented by Hirshfeld surfaces mapped with d_e, fullerene molecules as undecorated Hirshfeld surfaces, and the calixarenes by tube models.

(Figure 3b), and they make no contact on the other side (Figure 3a). Only two of the toluene molecules are intimately involved in the supermolecular structure; all remaining close contacts with the fullerene are made by neighbouring calixarene molecules in such a way that the supermolecules interdigitate with one another.

Figure 5 views the two supermolecules approximately down the pseudo-fivefold axis defined by the calixarenes, in this case with solvent molecules omitted. Figure 5a and c compare the bowl-shaped cavities of the calixarenes for the two complexes, and the uniform green-blue colour of the inner surfaces results from the close match between the curvature of the calixarene with that of the fullerene. The tops of the Hirshfeld surfaces of the fullerenes depicted in Figure 5b and d show the same smooth features, and these two figures also enable investigation of the contacts between the eclipsed arms of the calixarenes in the two cases. In $[C_{70}\subset\mathbf{2}_2]\cdot 7(C_7H_8)$ (Figure 5d) numerous C-H··H-C close contacts are identified by the orange-red spots on the surface of

the bottom calixarene, and in close proximity with hydrogen atoms of the top calixarene. This is not the case for $[C_{70}\subset\mathbf{1}_2]\cdot 6(C_7H_8)$, where there are almost no such contacts evident. The bonding nature of close hydrogen–hydrogen interactions in molecular crystals has been the topic of considerable recent discussion,[15,17] and the precise orientation of the calixarene arms with respect to one another in $[C_{70}\subset\mathbf{2}_2]\cdot 7(C_7H_8)$, and the close H···H contacts between them, strongly suggests that this is an attractive interaction in the present case.

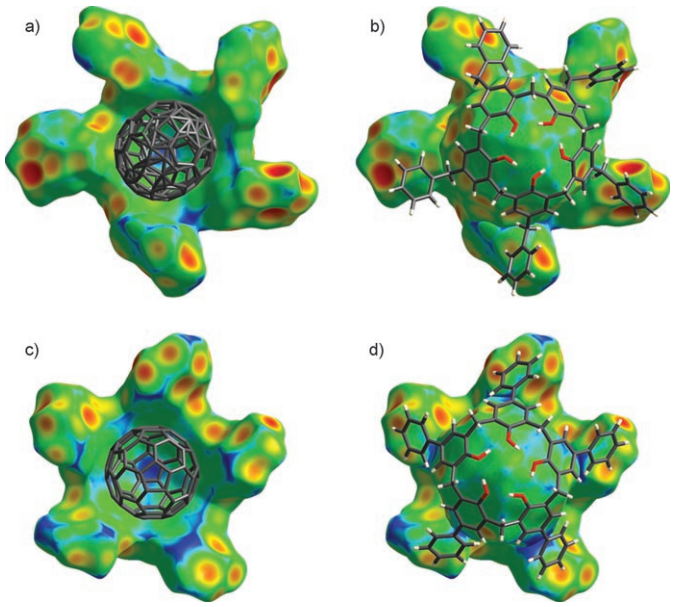

Figure 5. Hirshfeld surfaces for $[C_{70}\subset\mathbf{1}_2]\cdot 6(C_7H_8)$, (a) and (b), for $[C_{70}\subset\mathbf{2}_2]\cdot 7(C_7H_8)$, (c) and (d), showing cut away sections viewed down the axis of the "molecular capsules", with toluene molecules excluded.

Figure 6 compares Hirshfeld surfaces of the two C_{70} molecules. The surface in $[C_{70}\subset\mathbf{1}_2]\cdot 6(C_7H_8)$ reflects the nature of the close π···π contacts at the top and bottom, and the wide belt of numerous C–H···π contacts in the centre of the fullerene and between the two calixarene molecules, while for $[C_{70}\subset\mathbf{2}_2]\cdot 7(C_7H_8)$ there is evidence of only a small number of specific C-H···π contacts, and a greater area associated with π···π interactions. This is seen more directly from the fingerprint plots below each of Figure 6a and b. These plots are two-dimensional histograms of the relative frequency of points with individual (d_i, d_e) pairs on each of the Hirshfeld surfaces, d_i being defined analogous to d_e, but referring to the distance to the nearest nucleus internal to the surface.[9] Pixels associated with each pair of distances are coloured from blue (for very low frequency of occurrence), through green, to yellow and red (for highest frequency). There are two distinct regions in these plots, one resulting from large numbers of close contacts around $d_e \approx d_i \approx 1.8$ Å, and associated with π···π (or C···C) contacts, and the other near (d_i, d_e) ≈(1.8–2.0 Å, 1.3–1.5 Å), arising from the C-H···π (acceptor) contacts. Even the most cursory inspection of the fingerprint plots reveals that the fraction of surface area associated with these two broad contact types differs significantly between the two supermolecules, and a breakdown of the plots[18] confirms this: in $[C_{70}\subset\mathbf{2}_2]\cdot 7(C_7H_8)$ 41% of the fullerene Hirshfeld surface is involved in C···C contacts, and 59% in H···C contacts, while for $[C_{70}\subset\mathbf{1}_2]\cdot 6(C_7H_8)$ the fractions are 30 and 70%, respectively.

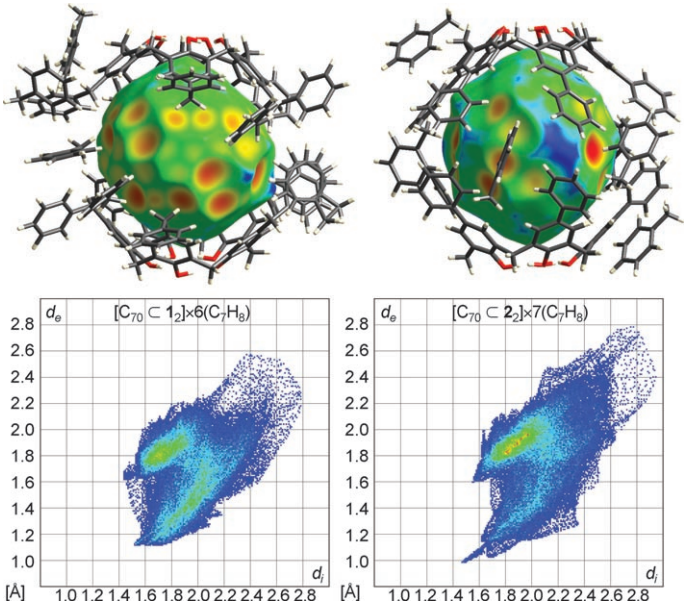

Figure 6. Hirshfeld surfaces for the fullerene molecules in $[C_{70}\subset\mathbf{1}_2]\cdot 6(C_7H_8)$ and $[C_{70}\subset\mathbf{2}_2]\cdot 7(C_7H_8)$, with 2D histograms (fingerprint plots) of the relative frequency of points on contact below each "molecular capsule".

Conclusion

We have established the interplay of non-spheroidal C_{70} with two calix[5]arenes, both with extended phenyl arms, but they differ in the ability of these arms to be involved in fullerene interactions in the host–guest complexes. While the complexes are similar in composition in having two calixarenes bound to the fullerene, they have remarkably different structures. The structure of $[C_{70}\subset\mathbf{1}_2]\cdot 6(C_7H_8)$ has additional calixarene interplay in the equatorial plane of the supermolecule, as well as solvent molecules. The fullerene is disordered, and this possibly reflects the less compact interplay of the components which is evident in the Hirshfeld surfaces. In $[C_{70}\subset\mathbf{2}_2]\cdot 7(C_7H_8)$ the fullerene snugly fits into the confines of the two calixarenes and five solvent molecules, in an intricate way involving C-H···π and π···π interactions, which is readily mapped out using Hirshfeld surfaces. Overall, we have shown that the use of Hirshfeld surfaces, now possible for disordered systems, is a very powerful tool in visualising and understanding the nature of interactions in large supramolecular systems, and is destined to be a versatile tool in providing valuable information regarding struc-

tural design, and understanding the nature of interaction of molecules, and more.

Experimental Section

General: All solvents and starting materials were obtained from Aldrich and used without further purification. *p*-Benzylcalix[5]arene (**1**) and *p*-phenylcalix[5]arene (**2**) were prepared according to the reported method.[11] NMR spectra were recorded on a 300 MHz Bruker DRX300 spectrometer. X-ray data was recorded on an Bruker AXS CCD diffractometer.

Preparation:

$[C_{70}\subset\mathbf{1}_2]\cdot 6(C_7H_8)$: To a solution of C_{70} (5 mg) in toluene (5 mL) was added **1** (11 mg). Slow evaporation over 2 d (to 1 mL) afforded reddish prisms which were collected and washed with toluene (0.5 mL) then hexane (2×1 mL). Yield: 6 mg (42%).

$[C_{70}\subset\mathbf{2}_2]\cdot 7(C_7H_8)$: To a solution of C_{70} (5 mg) in toluene (1 mL) was added **2** (11 mg). Slow evaporation over 2 d (to 1 mL) afforded dark-reddish needles which were collected and washed with toluene (0.5 mL) then hexane (2×1 mL). Yield: 6 mg (50%). As the crystals of the complexes were solvent dependent, microanalyses were not performed.

X-ray crystallography: The X-ray diffracted intensities were measured from single crystals at about 173 K on a Bruker CCD instrument using monochromatized $Mo_{K\alpha}$ ($\lambda = 0.71073$ Å). Data were corrected for Lorentz and polarization effects and absorption correction applied using multiple symmetry equivalent reflections. The structures were solved by direct methods and refined on F^2 using the Bruker SHELXTL crystallographic package. A full matrix least-squares refinement procedure was used, minimizing $w(F_o^2 - F_c^2)$, with $w = [s^2(F_o^2) + (AP)^2 + BP]^{-1}$, where $P = (F_o^2 + 2F_c^2)/3$. Agreement factors ($R = \Sigma||F_o| - |F_c||/\Sigma|F_o|$, $wR2 = \{\Sigma[w(F_o^2 - F_c^2)^2]/\Sigma[w(F_o^2)^2]\}^{1/2}$ and GOF $= \{\Sigma[w(F_o^2 - F_c^2)^2]/(n-p)\}^{1/2}$ are cited, where n is the number of reflections and p the total number of parameters refined). Because of the solvent dependency of the crystals, three additional unit cell collections were performed on randomly selected crystals to confirm the content of the bulk material for each complex.

Crystal and refinement details for $[C_{70}\subset\mathbf{1}_2]\cdot 6(C_7H_8)$ (1 = *p*-benzylcalix[5]arene); formula C_{70}, $2(C_{70}H_{60}O_5)$, $6(C_7H_8)$: $C_{252}H_{168}O_{10}$, $M = 3355.86$, $F(000) = 7040e$, monoclinic, $P2_1/c$, $Z = 4$, $T = 173$ K, $a = 19.927(2)$, $b = 29.458(4)$, $c = 28.591(4)$ Å, $\beta = 92.509(2)°$, $V = 16767(4)$ Å^3; $\rho_{calcd} = 1.329$ g cm^{-3}; $\sin\theta/\lambda_{max} = 0.6838$; N(unique) = 41780 (merged from 151639, $R_{int} = 0.044$, $R_{sig} = 0.054$), N_o ($I > 2s(I)$) = 26691; $R = 0.0920$, $wR2 = 0.2231$ (A,$B = 0.11$, 19.4), GOF = 1.066; $|\Delta\rho_{max}| = 1.0(1)$ e Å^{-3}.

Crystal and refinement details for $[C_{70}\subset(\mathbf{2})_2]\cdot 7(C_7H_8)$ (2 = *p*-phenylcalix[5]arene); formula C_{70}, $2(C_{65}H_{50}O_5)$, $7(C_7H_8)$: $C_{249}H_{156}O_{10}$, $M = 3307.74$, $F(000) = 6920e$, monoclinic, $P2_1/c$, $Z = 4$, $T = 173$ K, $a = 18.101(9)$, $b = 18.240(9)$, $c = 50.52(3)$ Å, $\beta = 91.202(9)°$, $V = 16675(14)$ Å^3; $\rho_{calcd} = 1.318$ g cm^{-3}; $\sin\theta/\lambda_{max} = 0.5946$; N(unique) = 27403 (merged from 98054, $R_{int} = 0.188$, $R_{sig} = 0.244$), N_o ($I > 2s(I)$) = 12513; $R = 0.1100$, $wR2 = 0.2281$ (A,$B = 0.12$, 112.39.4), GOF = 0.99; $|\Delta\rho_{max}| = 0.6(1)$ e Å^{-3}.

CCDC-617754 ($[C_{70}\subset\mathbf{1}_2]\cdot 6(C_7H_8)$) and -617755 ($[C_{70}\subset(\mathbf{2})_2]\cdot 7(C_7H_8)$) contain the supplementary crystallographic data for this paper. These data can be obtained free of charge from The Cambridge Crystallographic Data Centre via www.ccdc.cam.ac.uk/data_request/cif.

Hirshfeld surface analysis: Hirshfeld surfaces and fingerprint plots were produced with CrystalExplorer[19] with bond lengths to hydrogen atoms set to standard values.[20] Orientational disorder of the type encountered in these structures can be treated in two ways: i) defining the Hirshfeld surface incorporating fractional occupancies of the atoms; or ii) examining surfaces and plots due to each of the possible molecular orientations in turn. The results differ little, and all plots in Figures 3–6 were produced using the first method.

Acknowledgement

This work was supported by the Australian Research Council.

[1] M. Makha, A. Purich, A. N. Sobolev, C. L. Raston, *Eur. J. Inorg. Chem.* **2006**, 507–517.
[2] M. Makha, C. L. Raston, A. N. Sobolev, P. Turner, *Cryst. Growth Des.* **2005**, *6*, 224–228.
[3] J. L. Atwood, G. A. Koutsantonis, C. L. Raston, *Nature* **1994**, *368*, 292–295.
[4] J. L. Atwood, L. J. Barbour, P. J. Nichols, C. L. Raston, C. Sandoval, *Chem. Eur. J.* **1999**, *5*, 990–996.
[5] P. J. Nichols, C. L. Raston, C. A. Sandoval, D. J. Young, *Chem. Commun.* **1997**, 1839–1840.
[6] M. Makha, M. J. Hardie, C. L. Raston, *Chem. Commun.* **2002**, 1446–1447.
[7] M. A. Spackman, P. G. Byrom, *Chem. Phys. Lett.* **1997**, *267*, 215–220.
[8] J. J. McKinnon, A. S. Mitchell, M. A. Spackman, *Chem. Eur. J.* **1998**, *4*, 2136–2141.
[9] M. A. Spackman, J. J. McKinnon, *CrystEngComm* **2002**, *4*, 378–392.
[10] J. J. McKinnon, M. A. Spackman, A. S. Mitchell, *Acta Crystallogr. Sect. B* **2004**, *60*, 627–668.
[11] M. Makha, C. L. Raston, B. W. Skelton, A. H. White, *Green Chem.* **2004**, *6*, 158–160.
[12] M. Makha, C. L. Raston, A. N. Sobolev, L. Barbour, P. Turner, *CrystEngComm* **2006**, *8*, 306–308; M. Makha, C. L. Raston, A. N. Sobolev, *Aust. J. Chem.* **2006**, *59*, 260–262.
[13] J. L. Atwood, L. J. Barbour, M. W. Heaven and C. L. Raston, *Chem. Commun.* **2003**, 2270–2271.
[14] I. Dance, M. J. Scudder, *J. Chem. Soc. Dalton Trans.* **1998**, 3155–3165.
[15] C. F. Matta, J. Hernández-Trujillo, T. H. Tang, R. F. W. Bader, *Chem. Eur. J.* **2003**, *9*, 1940–1951.
[16] F. Cortes-Guzman, J. Hernandez-Trujillo, G. Cuevas, *J. Phys. Chem. A* **2003**, *107*, 9253–9256.
[17] E. Zhurova, V. G. Tsirelon, V. V. Zhurov, A. I. Stash, A. A. Pinkerton, *Acta Crystallogr. Sect. B* **2006**, *62*, 513–520.
[18] J. J. McKinnon, M. A. Spackman, unpublished results..
[19] S. K. Wolff, D. J. Grimwood, J. J. McKinnon, D. Jayatilaka, M. A. Spackman, CrystalExplorer 1.6, **2006**, University of Western Australia (http://www.theochem.uwa.edu.au/CrystalExplorer).
[20] F. H. Allen, O. Kennard, D. G. Watson, L. Brammer, A. G. Orpen, R. Taylor, in *International Tables for Crystallography, Vol. C* (Ed.: A. J. C. Wilson), Kluwer Academic, Dordrecht, **1995**, pp. 685–706.

Received: August 16, 2006
Revised: November 28, 2006
Published online: February 26, 2007

